Results in Engineering 24 (2024) 102919

Contents lists available at ScienceDirect

Results in Engineering

journal homepage: www.sciencedirect.com/journal/results-in-engineering

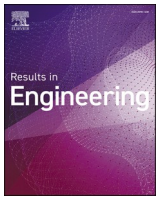

# Development and experimental performance evaluation of a small-scale aquavoltaic system for microalgae production

Hooman Pirtaj Hamedani [b], Shiva Gorjian [a,b,*], Barat Ghobadian [b], Hamed Mokhtarzadeh [b]

[a] Fraunhofer Institute for Solar Energy Systems ISE, Heidenhofstraße 2, 79110, Freiburg im Breisgau, Germany
[b] Biosystems Engineering Department, Faculty of Agriculture, Tarbiat Modares University (TMU), P.O. Box: 14115-111, Tehran, Iran

ARTICLE INFO

*Keywords:*
Aquaculture
Solar energy
Raceway open pond
Microalgae
Optimization

ABSTRACT

The primary objective of this study is to develop a small aquavoltaic system and evaluate key parameters, including dissolved oxygen (DO), pH, water temperature and dead zones in an open raceway pond to improve the conditions for the production of microalgae while generating electricity. The key variable parameters examined were the rotation speed of a paddle wheel at 10, 20 and 30 rpm, water depth at 15, 25 and 35 cm and response time at 0.5, 1 and 1.5 h were evaluated during May 9–15, 2023. Response Surface Methodology (RSM) and Central Composite Design (CCD) were used to optimize these parameters for acheiving DO levels suitable for microalgae production. The findings showed that increasing the rotation speed of a paddlewheel at the appropriate water depth significantly influences the flow rate, thereby controling DO levels. A maximum DO value of 6.94 mg/l was achieved after 1 h at a water depth of 25 cm and the paddle wheel rotation speed of 20 rpm. Increasing the rotation speed from 10 to 30 rpm resulted in DO values within the optimal range of 6–7 mg/l, reducing dead zones from 21.05 % to 9.16 %. However, with a paddle wheel spinning at 10 rpm, DO decreased below 5 mg/l with increasing water depth and minimal shading, with pH reaching a minimum of 6.8 ppm. Addiotionally, the experiments revealed no significant difference in efficiency between modules installed in open ponds and those installed on the ground over short time periods. The economic analysis indicated that spirulina production costs are 7 % higher with the non-aquavoltaic system due to non-solar electricity use. Furtehrmore, the cost of spirulina produced with the aquavoltaic system was 0.4975 USD/g at a 5 % interest rate and 0.331 USD/g at a 10 % interest rate in the fifth year. The current study underlines that aquavoltaics could have the potential to further increase the production of microalgae and thus reduce production costs. This opens up opportunities for long-term research leading to further optimization between energy production and environmental sustainability in aquaculture systems.

| Symbol | Unit |
|---|---|
| dz | Percentage of dead zones, % |
| $V_v$ | Volume of fluid in the dead zones, $m^3$ |
| $V_t$ | Volume of working fluid in the open raceway, $m^3$ |
| ρ | Fluid density, $kg/m^3$ |
| u | Fluid velocity in the channel, m/s |
| $R_h$ | Hydraulic radius in the channel, m |
| μ | Viscosity of the fluid, Pa.s |
| $R_e$ | Reynolds number, - |
| $w_c$ | Width and d for the depth of the channel, m |
| D | Diameter of the paddlewheel, m |
| N | Rotational speed of the paddlewheel, rpm |
| $P_0$ | Dimensionless power number, - |

(*continued on next column*)

(*continued*)

| Symbol | Unit |
|---|---|
| W | Power, watts |
| $P_a$ | Actual power required for the paddlewheel, watts |
| $M_r$ | Torque of the motor, N.m |
| T | Torsional torque transmitted from the motor to the shaft, N.m |
| $F_s$ | Drag force exerted by the fluid, N |
| $M_{bs}$ | Bending moment caused by the Newton meter drag force, N.m |
| $L_{sh}$ | Shaft length, m |
| $D_{sh}$ | Shaft diameter, m |
| $\tau_{max}$ | Maximum shear stress, Pa |

* Corresponding author. Fraunhofer Institute for Solar Energy Systems ISE, Heidenhofstraße 2, 79110, Freiburg im Breisgau, Germany.
*E-mail addresses:* shiva.gorjian@ise-extern.fraunhofer.de, Gorjian@modares.ac.ir (S. Gorjian).

https://doi.org/10.1016/j.rineng.2024.102919
Received 16 July 2024; Received in revised form 5 September 2024; Accepted 16 September 2024
Available online 25 September 2024

## 1. Introduction

Aquaculture, the farming of aquatic organisms such as fish, shellfish, and aquatic plants, is indeed of great importance to the food industry. It plays a crucial role in meeting the growing global demand for seafood and provides a sustainable source of protein for human consumption [1, 2]. Aquaculture is closely linked to many of the SDGs. It supports SDG 2 (Zero Hunger) through its ability to ensure a sustainable supply of proteins that are critical to global food security. By increasing seafood production and reducing pressure on wild fish stocks, aquaculture ensures access to nutritious food for a growing population [3]. SDG 7 (Affordable and clean energy) is addressed through the integration of renewable energy sources in aquaculture facilities. This switch not only reduces operating costs, but also promotes energy sustainability in the industry [4,5]. SDG 13 (climate action) is also linked to aquaculture, as the industry reduces greenhouse gas (GHG) emissions. In addition, the production of microalgae plays a key role in this aspect of climate protection.

Aquaculture facilities are known for their high energy consumption which accounts for around 40 % of total energy costs [6]. The geographical location, the type of species farmed, and the design of the system together play a crucial role in determining the energy consumption of an aquaculture system. Approximately 0.5 % of global GHG emissions can be attributed to aquaculture. While fossil fuels, diesel, and oil are common energy sources utilized in aquaculture industry, it is important to note that there are sustainable alternatives that are being explored to reduce the industry's reliance on non-renewable resources [4]. The expansion and improvement of existing aquaculture facilities can increase production, but also require the creation of new facilities, leading to increased competition for feed, space, water, energy, and resources [7]. Aquavoltaic systems are innovative systems that combine photovoltaics with aquaculture or water-based systems. These systems use the surface of bodies of water to install photovoltaic (PV) panels, enabling the simultaneous production of electricity and other valuable aquatic products. In addition to the simultaneous generation of solar power and aquatic farming, aquavoltaics offers benefits such as optimal water utilization and a suitable replacement for the fossil fuel-based aquaculture industry. This dual approach can significantly meet the communities' needs for water, food, and energy [8] (Boyd et al., 2021; [7]).

Microalgae are highly efficient at sequestering $CO_2$, which makes them a valuable tool in reducing the carbon footprint of aquaculture operations. In addition, the cultivation of microalgae in open pond systems, when integrated with PV technology, can improve energy efficiency, and reduce water evaporation, further aligning aquaculture practices with climate change mitigation goals [9]. Microalgae are promising for aquaculture due to their high content of high-quality proteins, essential fatty acids, pigments, and other vital nutrients [10]. As feed for aquatic organisms, microalgae offer a better amino acid profile than fishmeal and other animal-based feeds [11]. In addition, microalgae can help purify aquaculture water and maintain microbial balance. Consequently, microalgae can be used not only as a food source for aquatic animals, but also to improve the overall health and sustainability of aquaculture facilities. Currently, more than 20 genera and 40 species of microalgae, including golden algae, diatoms, and green algae, are widely used as aquatic feed [12]. Research into microalgae has attracted a lot of attention due to their many potential applications [13]. Like other microorganisms, e.g., bacteria or fungi, suitable culture conditions are required for the productivity and growth rate [14]. In this respect, the most important parameters are light, nutrients, pH value, temperature, and oxygen ($O_2$) content, which must be supplied correctly to the cells [15]. Currently, microalgae can be produced under field conditions either in open pond systems or in closed photobioreactors (PBRs) due to their identified properties. The cultivation of microalgae is primarily carried out in open pond systems, i.e., in open circular channels in which a flow of liquid is generated by mechanical agitation with a paddle wheel [16]. Cultivation in open raceway ponds offers the simplest and cheapest approach for the phototropic production of microalgae. The essential parameters for microalgae production in open raceway pond systems include water temperature, light availability, $O_2$ content and pH. However, the most important parameter for successful microalgae production is the DO of the water. A high DO can lead to respiratory problems with microalgae [7]. In open ponds, DO levels reach saturation due to the exchange between the aquatic environment and the atmosphere. This physical process depends largely on the exchange between the water and the air surface which is mainly influenced by the wind flow. In addition, the DO concentration in water is influenced by temperature, water depth and seasonal and diurnal cycles. As temperature increases, the solubility, saturation concentration of $O_2$ and the ability to retain it in the water decrease. The most important factor in increasing and controlling $O_2$ levels within the acceptable range for microalgae production in open raceway pond systems is the use of mixing systems that generate adequate velocity and flow, improve vertical mixing, and circulate the water [16]. Appropriate stirring affects essential parameters of microalgae production, such as $O_2$ content, and prevents sedimentation in the diluted solution [4]. It also reduces dead zones in raceway ponds. These stagnant areas in raceway ponds lead to an accumulation of solids and unnecessary energy loss [17]. Various experiments show that shading, especially in the warm seasons by installing solar panels, can influence the water temperature and thus the DO levels. However, the integration of solar panels can also be an advantageous alternative to shading nets. In this case, the stress caused by high temperatures is reduced and the daily temperature fluctuations in the open pond are minimized [18]. Hadiyanto et al. [19] reduced dead zones from 18 % to 3 % by changing the aspect ratio of a channel basin and maintaining a flow velocity of 0.15–0.30 m per second in a computational fluid dynamics (CFD) simulation. Lauguico et al. [20] measured the DO based on the primary cultivation parameters of microalgae using machine learning models. Based on available data, the standard range for DO in a microalgae cultivation environment was between 6 and 7 mg/l. Amin et al. [21] conducted a research study using machine learning techniques to optimize DO levels in several microalgae farms. The machine learning model Support Vector Regression (SVR) predicted the range of DO in water to be 5.5–5.6 mg/l, with a negligible error percentage compared to actual values. A study by Matulić et al. [9] explored the integration of solar PV systems with aquaculture in Croatia, emphasizing the benefits of dual land use. This study highlights that installing PV panels over water bodies reduces water evaporation and provides shade, leading to cooler microclimates that benefit aquatic life and enhance PV efficiency. The study emphasized that while initial costs are high, the long-term benefits include reduced water needs and increased yields, which are critical in addressing the challenges posed by climate change and land scarcity. Château et al. [22] Click or tap here to enter text. Investigated a dynamic model to study the primary biochemical processes in a fish farm pond covered with floating photovoltaic (FPV) panels. The results showed that FPV arrays can have an impact on some of the essential parameters of the aquaculture environment, such as the reduction of DO in the water. However, the energy obtained from this integration is significant and can compensate for the losses in fish production. In another study, Kim et al. [23] proposed a FPV system for combined salt harvesting and electricity generation. They found that temperature and water depth have different effects on the performance of the modules and do not correlate strongly with each other. Furthermore, the results indicated that the short-term performance of the PV modules will not be influenced by the salinity of the seawater. They confirmed that the electrical output of the FPV system is better than that of the ground-mounted (GM) solar panels due to the cooling effect of the panels located near the water. The enhanced efficiency of PV panels when integrated with aquatic systems is further supported by Hu et al. [24]. Their review categorizes water-based PV systems into fixed pile, floating, floating platform, and floating photovoltaic tracking systems. The cooling effect of water bodies was found to

enhance the performance of PV panels by maintaining lower operating temperatures. They explained this not only increases energy yield but also extends the lifespan of the panels. The study emphasized the need for robust mooring systems to adapt to water level changes and avoid horizontal movement, which is crucial for the stability and efficiency of FPV systems. Imani et al. [5] explored the feasibility of using solar-powered aeration systems in shrimp farms in western Taiwan. Through simulations, the study designed a solar-powered system capable of fully meeting the energy demands of a small-scale shrimp farm. The results indicated that with an average monthly energy production of 32 MWh, the system could effectively support the power needs of the shrimp farm, ensuring continuous production and reducing reliance on non-renewable energy sources. In another study, Trapani and Millar [25] installed a small thin-film laboratory PV system on the surface of an outdoor swimming pool in Sarnia, Canada. Test results over 45 days showed a 5 % increase in electricity production due to the cooling effect of the water over three months. Bautista-Monroy et al. [4] conducted a study in a raceway pond to investigate the effects of rotation speeds of 35, 40, and 45 rpm on dead zones. The dead zones were 13.4 %, 7.93 %, and 4.16 %, respectively. The results showed that increasing the rotation speed reduces dead zones in raceway ponds for microalgae production. Vo et al. evaluated the integration of solar energy within aquaculture, highlighting its potential to address the high energy demands of this industry, which constitute approximately 40 % of total operational costs. The study reviewed several applications of solar energy in aquaculture across different companies worldwide, demonstrating its effectiveness in reducing energy costs and enhancing sustainability. In another study, Vo et al. [26] outlined how combining PV energy with aquaculture can alleviate some of the major problems facing the aquaculture industry in desert regions. One major problem, they explained, is the high energy consumption in aquaculture, particularly for tasks such as water aeration and temperature control, which are essential for maintaining optimal conditions for fish and other aquatic organisms. They claimed that by using solar energy, these energy-intensive processes can be run sustainably, reducing dependence on fossil fuels, and lowering operating costs.

A significant research gap in the field of aquavoltaics lies in the nuanced understanding of the interaction between PV systems and DO levels in aquatic environments, particularly in open raceway pond systems. While the integration of PV technology into aquaculture is gaining more and more attention, the effects of PV systems on oxygen concentration are still insufficiently researched and often contradictory. Existing studies are limited in scope and often focus on single variables, leading to contradictory conclusions. For example, some studies suggest that PV systems can increase DO levels due to shading effects that mitigate excessive solar radiation [27]. In contrast, other studies argue that PV systems can reduce DO concentrations by altering wind patterns and increasing water temperature due to the obstruction of natural air circulation [22]. This divergence underscores the urgent need for comprehensive research that considers the multifactorial influences of PV systems, including shading, wind dynamics, temperature fluctuations and their cumulative effects on oxygen levels. Addressing this gap is critical for optimizing PV systems to improve aquatic productivity and sustainability while protecting water quality and the health of aquatic organisms. Future research should aim to develop a more comprehensive understanding of these complex interactions to enable the development of more efficient and environmentally friendly aquavoltaic systems.

Another critical gap in the literature is the economic analysis of aquavoltaic systems, in particular their scalability and cost-effectiveness under different geographical and climatic conditions. Current research often focuses on the technical aspects, but there is a need for more comprehensive studies that assess the financial feasibility, potential economic benefits, and barriers to widespread adoption of aquavoltaic technologies, especially in regions with different economic constraints. Aquavoltaics represents a fundamental solution to several pressing challenges, including the high energy demand of microalgae production, the need to minimize the use of agricultural land, the multifunctional use of resources and the control of evaporation during droughts. Aquavoltaics also plays a crucial role in reducing fossil fuel consumption and associated emissions. However, despite its potential, several critical research gaps remain under-researched, particularly in understanding the nuanced interactions between PV systems and various environmental factors in aquaculture. To address these issues, this study developed and evaluated an aquavoltaic system specifically tailored to investigate key factors affecting the aquaculture environment, with a focus on microalgae cultivation. These factors include DO, light exposure, pH, and water temperature. Using the response surface method (RSM), this study attempts to determine optimal DO levels while minimizing stagnant areas in open pond systems. This optimization process involves fine-tuning the input parameters to improve the results of microalgae cultivation. By addressing the identified gaps, such as economic viability and wider water quality impacts, this research aims to contribute to the holistic development of sustainable and efficient aquaculture systems.

## 2. Materials and methods

### 2.1. Description of the proposed aquavoltaic system

A schematic representation of the open raceway pond utilized in this study is shown in Fig. 1. The components of the small-scale aquavoltaic system utilized in this research include: (i) an open raceway pond, (ii) a mechanical paddle wheel, (iii) a motor and power transmission system, (iv) a motor speed control circuit, and (v) a photovoltaic system. Open raceway ponds are usually designed for the large-scale cultivation of microalgae. These ponds are usually shallow, rectangular channels in which the water containing the microalgae circulates continuously to provide nutrients and sunlight for growth. The open design allows easy access to sunlight and air, but also presents challenges such as evaporation and contamination. Closed-loop systems, on the other hand, are designed to circulate water within a closed system to minimize water loss and create optimal growth conditions for the microalgae [16]. In this study, it was found that the optimum water depth for microalgae production in the open raceway pond is around 0.3 m. By controlling this specific water depth together with other parameters such as rotation speed and reaction time, it is possible to create favorable conditions for both microalgae production and electricity generation in the aquavoltaic system [28]. Polyethylene was selected as the material for

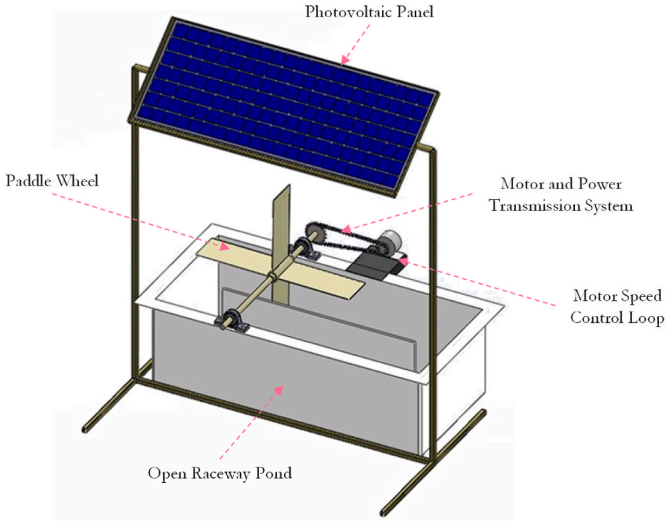


**Fig. 1.** Schematic view of a small-scale aquavoltaic system developed in this study.

building the raceway pond due to its superior durability and ability to withstand direct sunlight. The recommended length to width ratio for the open pond used in small-scale microalgae production typically falls between 2 and 2.5 [29]. The middle partition is 15 mm thick, and its length is about 12 %–15 % less than the total length of the open raceway pond.

### 2.2. Realizing the dead zones in the open raceway pond

Dead zones in raceway ponds have a detrimental impact on fluid dynamics and mixing, causing stagnation and the buildup of solids, resulting in energy wastage [17]. In these ponds, even with just a single middle baffle, dead areas exist (see Fig. 1A[1]). In this case, computational fluid dynamics (CFD) was utilized to simulate flow patterns and dead zones in open raceway ponds with a length-to-width ratio of 2.5 at different velocities. The dead zones were determined based on volume fraction and are computed using Eq. (1) [4]:

$$\%dz = \frac{V_v}{V_t} \cdot 100 \tag{1}$$

$$V_t = A_{Raceway} \cdot h_{Fluid} \tag{2}$$

Where dz represents the percentage of dead zones (%), $V_v$ represents the volume of fluid in the dead zones ($m^3$), and $V_t$ represents the volume of working fluid in the open raceway pond ($m^3$), calculated using Eq. (2). In this equation, A is the pond area in square meters and h is the liquid height in the pond in meters. A digital anemometer was used to measure the fluid flow velocity. The volume of fluid in the dead zones was also approximated at flow rates of 10, 20, and 30 rpm, and the results were obtained. A flat vane impeller with four vanes was designed and constructed to generate fluid flow and mixing. The turbulence of the flow depends on the Reynolds number (Re) and can be calculated using Eq. (3) [16].

$$R_e = \frac{\rho u R_h}{\mu} \tag{3}$$

Where ρ is the fluid density in $kg/m^3$, u is the fluid velocity in the channel in m/s, Rh is the hydraulic radius in the channel in meter, and μ is the viscosity of the fluid (Pa.s). The density and viscosity of water are like that of a dilute solution of microalgae in water [28]. The hydraulic radius depends on the geometry of the channel and can be calculated using Eq. (4).

$$R_h = \frac{dw_c}{w_c + 2d} \tag{4}$$

In this equation, $w_c$ stands for the width and d for the depth of the channel in meters.

### 2.3. Design of the paddle wheel and power transmission system

The power required for the paddle wheel depends on the flow velocity [28]. In general, the fluid for microalgae production in open raceway ponds requires a minimum velocity of 0.3 m/s [17]. The actual power required for the paddlewheel can be calculated using Eq. (5) [30].

$$P_a = p_0 \rho N^3 D^5 \tag{5}$$

Where D represents the diameter of the paddlewheel in meters, N represents the rotational speed of the paddlewheel in revolutions per second, ρ represents the density of the fluid in $kg/m^3$, $P_0$ represents the dimensionless power number, and W represents the power in watts. The power number is determined based on the Reynolds number, which is calculated to be 245,000 in this study. The power number of 1.3 is considered [31]. The power produced by the engine should not only meet the power requirements of the paddlewheel, but also consider the losses through the gearbox and bearings. Since the fluid has a low viscosity, the final power requirement is calculated using Eq. (6):

$$P_a' = 1/5 P_a \tag{6}$$

The torque of the motor is calculated with Eq. (7).

$$M_r = \frac{P_a'}{2\pi N} \tag{7}$$

In this equation, the torque is measured in newton-meter. The "Engineering Equipment Users Association" (EEUA) method was used to design the shaft [31]. In general, the theory behind this method is based on securing the paddlewheel and considering the motor as a stationary element. The torsional torque transmitted from the motor to the shaft can be calculated using Eq. (8).

$$T = n_t \times M_r \tag{8}$$

This equation assumes that $n_t$ is 1.5 at light work operating conditions [31]. T represents the torsional moment acting on the shaft in N.m. Assuming that the drag force Fs acts at a distance of 3/4 of the length of the propeller blade, Eq. (9) can be used:

$$F_s = \frac{8T}{3D} \tag{9}$$

In this equation, Fs is the drag force exerted by the fluid (N) and D is the diameter of the paddlewheel (m). The bending moment caused by the fluid drag force Fs acting along the shaft occurs at the end of the shaft connected to the motor and the bearing. This bending moment can be derived from Eq. (10).

$$M_{bs} = F_s \cdot L_{sh} \tag{10}$$

In this equation, Mbs is the bending moment caused by the Newton meter drag force, and $L_{sh}$ is the shaft length in meters. Based on the calculations, a torsional moment of 22.5 N m and a bending moment ($M_b$) of 26.36 N m were determined. Based on the design table, 37-gauge steel was selected as the material for the shaft. The yield stress of the steel is 235 MPa and the maximum shear stress is 180 MPa. Because the shaft is subjected to oscillating loads, a safety factor of 4 was considered. The shaft diameter was calculated to be 16 mm using Eq. (11) [32].

$$\frac{\pi}{16} \times \tau_{max} \times d_{sh}^3 = \sqrt{M_b^2 + T^2} \tag{11}$$

A gear and chain system was used as a power transmission unit (see Fig. 2A). Considering that the aquaculture system uses solar energy to power the open raceway pond electrical equipment for microalgae production, a DC motor with a gear ratio of 1:10 and a speed of 340

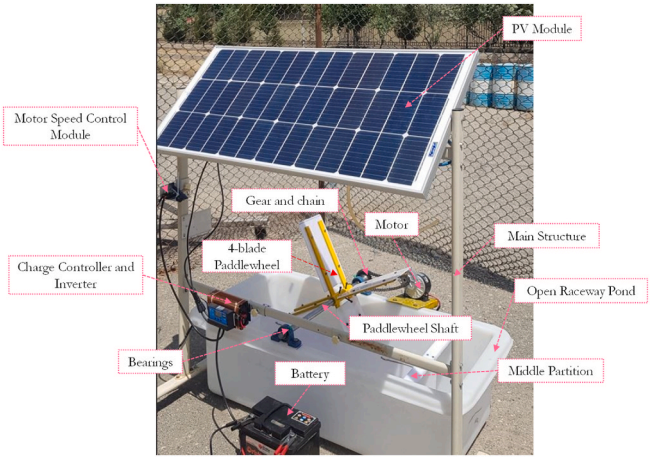


**Fig. 2.** Photo of the constructed aquavoltaic system.

[1] The figures are presented in Appendix.

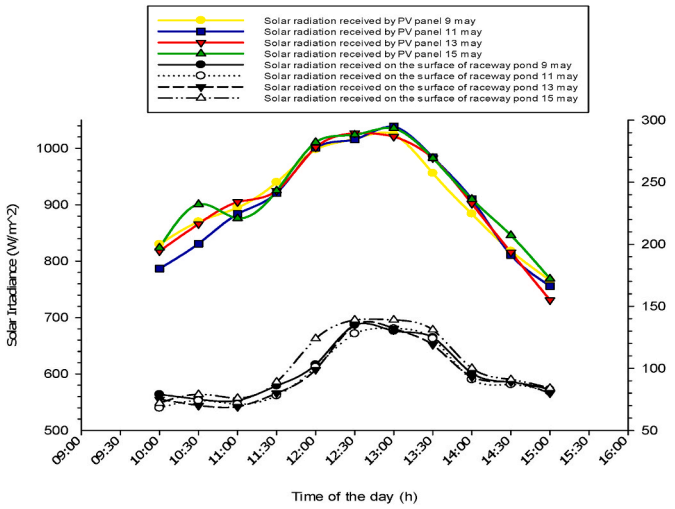


**Fig. 3.** Variations in solar radiation on the PV panel and the surface of the open pond during four evaluation days.

revolutions per minute (rpm) was used to provide the required power. The motor speed is controlled using pulse width modulation (PWM). The schematic representation of the speed control circuit is shown in Fig. 3A. This circuit uses the NE555 IC, the IRL535N MOSFET transistor for switching, the free-wheeling diode D3 and the potentiometer RV1. In this study, an off-grid PV system was designed and built to simultaneously generate electricity and power the aquaculture facility's electrical equipment. The system consists of silicon crystalline solar panels, specifically the EU-M100 model, with a nominal power of 100 W. The dimensions of the panels were tailored to the open pond to study the effects of shading on the main parameters of microalgae production. The frame of the panels was built from two profiles with dimensions 10 × 20 mm, height 130 cm and thickness 3 mm.

A 12-V battery with a capacity of 60 A-hours (Ah) and a 10-A charge controller were chosen for this system. The aquavoltaic system was placed at a latitude of 35.6 ° north and a longitude of 51.42 ° east, with an elevation of 1100 m above sea level. The constructed aquaculture system is shown in Fig. 2. During the daily experiments, solar radiation was measured with a solar power meter (model TES-1333). The measuring range of the device is 2000 W/m$^2$ meter and has a resolution of 1 W/m$^2$ meter, and it can measure solar radiation in the spectral range from 400 to 1100 nm. The radiation meter was positioned perpendicular to the surface of the solar panel, and the observed values were recorded. Radiation measurements were also taken below the panel and on the surface of the open pond to evaluate the difference in radiation intensity on the panel. Practical tests were conducted to investigate the effects of the defined variables on DO, water temperature, and pH in the raceway pond for microalgae production. For this purpose, a Taiwanese water quality meter (model WA2017SD) was used to measure DO, water temperature, and pH. The values were recorded and reported. The measuring range of the water quality meter for the DO is 0–20 mg/l with a resolution of 0.1 mg/l, for the temperature from 0 to 50 °C with a resolution of 0.1 °C and finally for the measurement of the pH value the range is 0–14 ppm.

### 2.4. Response surface methodology (RSM)

In the context of the aquavoltaic system in this study, utilizing RSM could have helped in determining the optimal combination of rotation speed, water depth, and reaction time to maximize the dissolved oxygen content for microalgae production. By systematically varying these factors and analyzing their effects on the outcome, researchers could have identified the ideal conditions for efficient microalgae growth [33]. Furthermore, RSM could have also been used to optimize the performance of the aquavoltaic system in generating electricity. By studying the relationship between variables such as solar intensity, paddle wheel speed, and electricity output, maximum power generation efficiency can be achieved. The first step in RSM is to determine the boundaries of the experimental area to be investigated. The process variables were optimized using the Central Composite Design (CCD) model, which consists of 19 runs with 5 repetitions at the central points. Paddlewheel speed, water depth and reaction time as seen in Table 1, using the values −1, 0 and + 1. The quadratic model is appropriate as it is based on three-level factors and blocking selection is provided for each scheme used [34]. The statistical software Design Expert 13 was used for the optimization and RSM analysis of the experimental data.

## 3. Results and discussion

### 3.1. Effect of environmental parameters and shading on DO

To evaluate the performance of the developed aquavoltaic system, the experimental tests were conducted during four days from May 9 to May 15, under different weather conditions, considering solar radiation, air temperature, and wind speed. However, in view of the minimal fluctuations in wind speed on the test days and the negligible differences between the values, the wind speed was excluded from the diagrams, and it was assumed that the conditions were stable. The experiments were conducted continuously from 9:00 in the morning until 16:00 in the afternoon. From 9:30 a.m., when the system had reached a stable state, the solar radiation, the air temperature, and the shadow effect created by the PV module were monitored. This was done to investigate the conditions of DO, the fluctuation of water temperature in the open raceway pond and the pH of the water. Solar radiation was measured every 30 min and, based on the data collected, the average solar radiation on May 9 and 13 was 909 W/m$^2$. In addition, the average solar radiation measured on May 11 was 904 W/m$^2$, while on May 15 it was 914 W/m$^2$. Furthermore, there were no significant fluctuations in air temperature on these days. In addition, the average solar radiation remained constant over the evaluation days. Therefore, the data from May 9 was selected for the system evaluation with the Design Expert software. The average fluctuations in available solar radiation and air temperature on the evaluation days is shown in Fig. 4A.

As shown in this figure, the solar radiation reaches its peak between 12:00 and 13:30. The decrease in solar radiation from 13:30 to 15:00 had no significant effect on the air temperature, which continued to show a steady upward trend from 10:00 to 15:00. Fig. 3 illustrates the variations in solar radiation received both above and below the solar panel, particularly on the surface of the open raceway pond. These fluctuations were considered as shading for the surface of the pond. As can be seen from the figure, the intensity of solar radiation increases between 12:00 and 13:30. As the PV panel is oriented at a 36-degree angle to the south, the amount of radiation on the surface of the racecourse pond increases. This increase in solar radiation leads to a reduction in the shadow cast by the solar panel on the surface of the pond. This phenomenon is attributed to the positioning of the PV panel at an angle of 36° to the midday sun. As a result, it was observed that the shadow cast by the panel decreased, and direct sunlight was able to reach the pond. Between 13:30 and 15:00, when the sun moves and the intensity of the solar radiation decreases, the degree of shading increases again.

**Table 1**
Designed and coded values of input parameters for RSM analysis.

| Variable | Units | Levels | | |
|---|---|---|---|---|
| | | −1 | 0 | 1 |
| **Depth of water** | cm | 15 | 25 | 35 |
| **Rotational speed** | rpm | 10 | 20 | 30 |
| **Reaction time** | h | 0.5 | 1 | 1.5 |

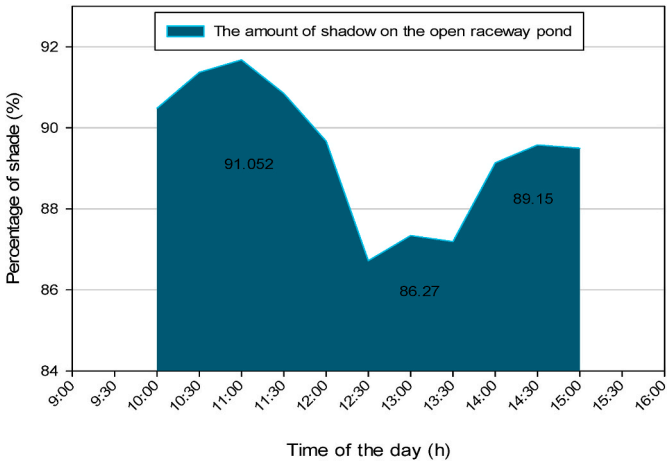


**Fig. 4.** Percentage of the shadow caused by the PV module on the surface of the pond.

The peak percentage of shading at the racecourse pond is observed between 10:00 and 11:30. During this period, the solar module is oriented at an angle of 36° to the south to capture the maximum sunlight, as the evaluation of the system shows. Fig. 4 shows the percentage of shade created by the solar panel over the raceway pond during the entire test period from 10:00 to 15:00. This shading helps to mitigate the daily temperature fluctuations both in the pond and under the PV solar panel. The resulting temperature equilibrium that is maintained throughout the day could potentially have a positive effect on the DO value. The average intensity of solar radiation, the temperature of the ambient air and the water temperature measured during the evaluation day (May 9, 2023) are shown in Fig. 5A. The temperature difference between the water and the ambient air was measured without the presence of a solar panel on the raceway pond. On average, the temperature difference was between 1 and 3 °C. The smallest temperature difference between the two environments was measured between 12:00 and 13:30, which coincides with the highest solar radiation of 1000 W/m$^2$. However, when a solar panel was placed on the surface of the raceway pond to provide shade, the temperature difference between the ambient air and the water increased to between 2 and 5 °C. This indicates that the PV system can significantly reduce the surface temperature of the water. The maximum temperature difference was observed between 13:30 and 15:00, when the air temperature reached its highest level. The smallest temperature difference was observed between 12:30 and 13:30. During this period, the movement of the sun and the increased radiation on the surface of the raceway pond combined with the reduced shading led to an increase in the water temperature. Fluctuations in the water temperature in the raceway pond can influence the DO. In addition, the lower water temperature between 10:00 and 11:30 was attributed to the maximum shading from the solar panels over the raceway pond. During the practical experiments, the DO in the water was measured without mixing, considering changes in water temperature. The water temperature fluctuates throughout the day due to the movement of the sun and the different irradiance levels in the open raceway pond. The shading effect of the PV module, which reduces the water temperature, can have a direct impact on the DO and pH performance.

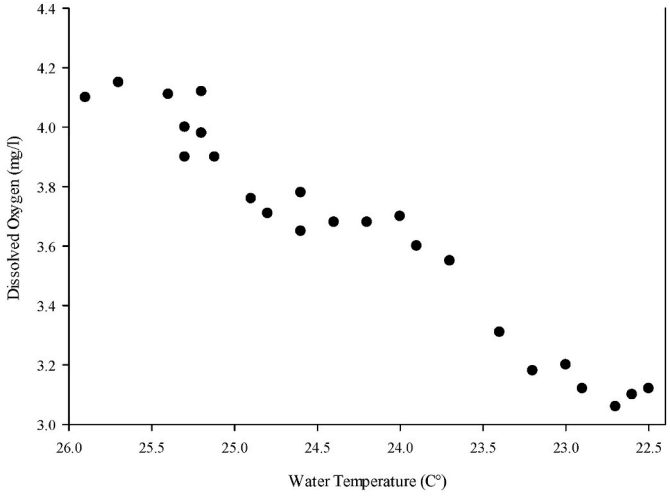


**Fig. 5.** Fluctuations in water temperature in the raceway pond and their effect on the DO during the day, without mechanical mixing by the paddle wheel.

Fig. 5 shows the relationship between the DO and the fluctuations in water temperature. There is a close correlation between the DO and the temperature of the water. In general, the DO decreases as the water temperature in the racecourse pond decreases. Li et al. [35] demonstrated that DO levels were higher in the 25 %, 50 % and 75 % shading test groups than in the no shading test group, suggesting that adequate shading does not affect normal DO levels in a raceway pond. They also discovered that the diversity of algae species and biomass can reach the maximum when the shaded area is more than 75 %. At the same time, fish production was at its peak.

### 3.2. RSM analysis of operating parameters for microalgae production

The CCD method was used to optimize the variable factors for the input parameters of the aquavoltaic system with the aim of controlling the allowable range of DO which is required to produce microalgae in the open raceway pond. This method, used within the RSM, helps to determine the optimal conditions and interactions between the input variables.

Table 1 shows an RSM table with the experimental design and the coded factors for the input parameters, where the rotation speed of the paddlewheel varied between 10 and 30 rpm, the water depth varied between 15 and 35 cm and the response time varied between 0.5 and 1.5 h. The test plans were carried out with the CCD. As shown in Table 2, the rotation speed of the paddle wheel, the water depth and the reaction time were analyzed, and the table lists the DO as a function of these parameters. The results of the analysis of variance (ANOVA) show that variables A, B and C are statistically significant.

The effects of the responses entered and the significance of the model is shown in the analysis of variance (ANOVA) table, in which the predicted, adjusted, and $R^2$ variables have values of 0.6775, 0.8839, and

**Table 2**
Experimental results for input and output parameters.

| Input factors | | | Response | |
|---|---|---|---|---|
| **A: Depth of water (cm)** | B: Rotational speed (rpm) | C: Reaction time (h) | DO (mg/l) | DO dead zone (mg/l) |
| **35** | 10 | 0.5 | 5.27 | 4.85 |
| **15** | 30 | 0.5 | 5.3 | 5.53 |
| **15** | 10 | 0.5 | 6.32 | 4.8 |
| **25** | 20 | 1.5 | 6.72 | 5.3 |
| **15** | 30 | 1.5 | 6.28 | 5.4 |
| **35** | 10 | 1.5 | 5.04 | 4.8 |
| **35** | 20 | 1 | 6 | 5 |
| **25** | 20 | 1 | 6.58 | 5.03 |
| **25** | 30 | 1 | 6.76 | 5.21 |
| **25** | 20 | 0.5 | 6.37 | 5.3 |
| **25** | 20 | 1 | 6.57 | 5.09 |
| **35** | 30 | 0.5 | 6.15 | 5 |
| **15** | 20 | 1 | 6 | 5.2 |
| **25** | 20 | 1 | 6.67 | 5.1 |
| **25** | 20 | 1 | 6.63 | 5.08 |
| **25** | 20 | 1 | 6.9 | 5.2 |
| **35** | 30 | 1.5 | 6.4 | 4.96 |
| **25** | 10 | 1 | 5.91 | 4.59 |
| **15** | 10 | 1.5 | 6.3 | 4.9 |

0.9355 respectively [36]. The analysis of variance (ANOVA) table with values for the variables $R^2$, adjusted $R^{2,}$ and projected $R^2$ of 0.9355, 0.8839, and 0.6775, respectively, illustrates the effects of the input responses and the significance of the model. From the results, A, B, C, AB, BC, and $A^2$ are significant model terms. The lack of fit is not differ significantly from the pure error, as shown by an F-value of 2.32 for the lack of fit. There is a 21.76 % probability that such a high F-value is due to random noise.

A difference of less than 0.2 between the "Adjusted $R^{2\prime\prime}$ of 0.8839 and the "Predicted $R^{2\prime\prime}$ of 0.6775 indicates adequate agreement. In addition, the signal-to-noise ratio, which indicates reasonable accuracy, should ideally be above 4. A ratio of 14.511 means a reasonable signal and indicates that the software modeling is robust and accurately predicts the actual data. However, in order for a model to be considered adequate, the model reduction must validate and accept the statistical analysis, which is crucial for running an optimization process. Equation. (12) provides the final equation for the experimental parameters and real factors as determined by the software:

$$DO\ (mg/L) = 6.61 - 0.1340\ A + 0.2050\ B + 0.1330C + 0.41\ AB - 0.1175\ AC + 0.1850\ BC - 0.5421\ A^2 - 0.2071\ B^2 \quad (12)$$

The results of ANOVA show that the interaction factors - particularly the water depth, the rotational speed of the paddle wheel and the reaction time - have a significant influence on the DO (see Table 1A). Fig. 6A–a shows a strong correlation between the actual and predicted values, demonstrating close agreement between the experimental results and the software model predictions. The linear relationship between these values emphasizes the accuracy of the model. In particular, the rotation speed of the paddlewheel proves to be a key factor in increasing the oxygen content in microalgae production in open raceway ponds. According to Bux and Chisti [16], increasing the rotational speed of the agitator at an optimal depth is crucial for improving mixing and increasing the oxygen content required for microalgae cultivation in open ponds.

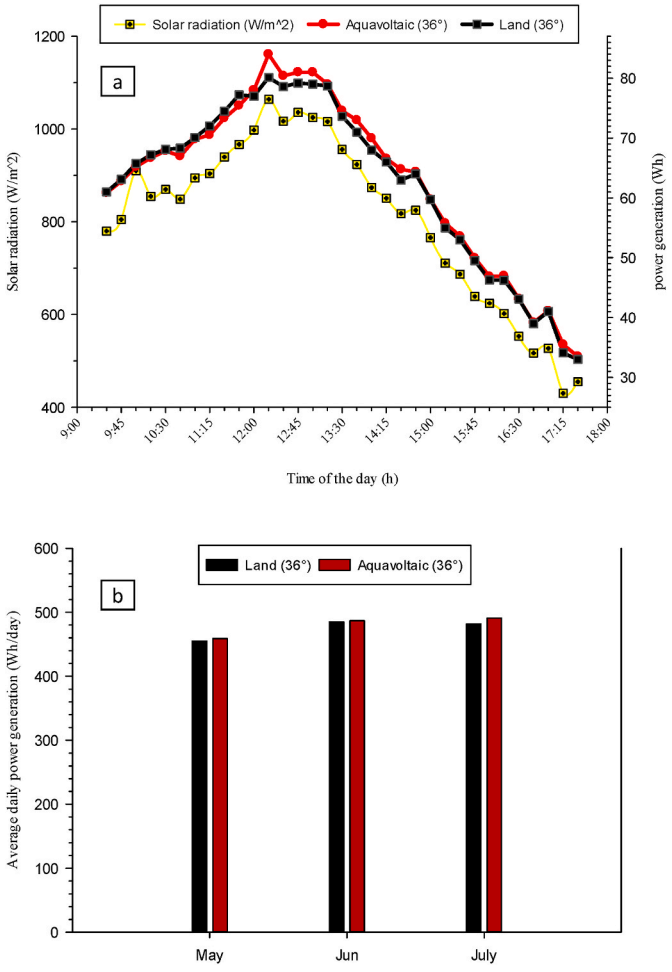


**Fig. 6. (a)** Comparison of power generation of ground-mounted and aquavoltaic modules on May 15, **(b)** Yield and power ratio of aquavoltaic and land module (May ~ July 2023).

In addition, Fig. 6A–b and **6A-c** show three-dimensional (3D) diagrams that illustrate the influence of the rotational speed of the paddle wheel on the DO. As shown in Fig. 6A–b, the DO decreases from 6.40 to 5.04 at a response time of 1 h, a rotating speed of the paddlewheel from 10 rpm to 30 rpm and a water depth of 35 cm. This observation confirms that at a water depth of 35 cm, the DO increases with higher rotational speeds of the mechanical paddlewheel. Furthermore, there is no significant influence of reaction time and water depth on the DO during the operation of the system. At a constant rotation speed of 30 rpm and a water depth of 15 or 35 cm, the amount of DO increases from 5.80 to 6.34 and reaches an upper constant value of 6.90. The results also confirm that at a paddlewheel rotation speed of 30 rpm and a water depth of 15–25 cm, the final amount of DO increases, while at a water depth of 25 cm–35 cm, a decreasing trend in the amount of DO is observed. The highest amount of DO in the water was thus reached at a speed of 20 rpm, a depth of 25 cm and a reaction time of 1 h. This simply proves that at optimum water depth and high paddle wheel speed the amount of DO increases, while at higher speed and water depth the amount of DO decreases. It can therefore be concluded from Fig. 6A–b that in the range of 25 cm water depth and 1.5 h reaction time, an increase in the speed of the mechanical paddle wheel leads to an increase in the DO of the water. Fig. 6A–c illustrates the effects of rotation speed and reaction time on the initial concentration of DO in the water. With a reaction time of 1.5 h and rotation speeds of 10 and 30 rpm, the DO increases from 6.15 to 6.88 mg/l. However, at a rotation speed of 30 rpm and reaction times of 1.5 and 0.5 h, the DO decreases from 6.88 to 6.32 mg/l. This phenomenon is because the rotation speed of the paddle wheel homogenizes the vertical water layers and increases the flow velocity of the liquid along the channel within a short reaction time. The DO along the flow path of the channel in the open pond shows a more stable performance over time. To summarize, as shown in Fig. 6A–c 13, at a fixed water depth of 35 cm and reaction times of 0.5 and 1.5 h, the DO increases with the rotation speed, increasing from 10 rpm to 30 rpm. In raceway ponds, A flow velocity of 0.3 m per second is often required for biomass production [28].

### *3.2.1. Analysis of DO in dead zones of open raceway ponds*

In an open raceway pond, the presence of a central partition creates dead zones, as shown in Fig. 1A. ANOVA was used to examine the variables affecting DO in the dead zones and the results are shown in Table 2A. The F value of 14.94 for the DO model of the dead zone means that the model is significant, although the probability that such a high F value is due to random noise is less than 0.01. P-values below 0.05 emphasize the significance of the model terms. In this case, the terms A, B, AB and B2 are crucial. The lack of fit is not significant when looking at the pure error, as the F-value of 3.65 shows. The probability that noise is responsible for a high F-value in the absence of fit is 11.23 %. If the model closely matches reality, the lack of fit should not be significant. A significant lack of fit indicates that the model is important and accurately predicts the actual data. In this part of the study, the $R^2$ value was determined to be 0.8518, which means that the regression model deviated from the experimental results by 14.85 %. The "adjusted $R^{2\prime\prime}$ value was also high at 0.7948, meaning that the model was highly significant. Furthermore, the "Predicted $R^{2\prime\prime}$ value of 0.7023 aligns closely with the "Adjusted $R^{2\prime\prime}$ value of 0.7948, with a difference of less than 0.2, indicating that the model is valid and reliably predicts the actual data. The equation resulting from the analysis is as follows:

$$\text{Dead Zone DO (mg/L)} = 5.14 - 0.1220\,A + 0.2160\,B - 0.0120C - 0.1150\,AB - 0.1404\,B^2 \quad (13)$$

As can be seen in Fig. 7A–a, there is a linear relationship between the predicted values and the calculated values for the DO in a dead zone. In addition, Fig. 7A–b which is a 3D plot of the response surface of rotation speed and water depth for the DO in the dead zones, indicates that with a reaction time of 1 h, a rotation speed of 30 rpm and a water depth of 15 cm and 35 cm, the DO in the dead zones decreased from 5.45 to 4.99. The results show that at a rotation speed of 30 rpm, an increase in water depth reduces the optimal fluid flow throughout the channel path and increases the percentage of dead zones in the open pond. Furthermore, at a fixed reaction time and a water depth of 15 cm, increasing the rotation speed from 10 rpm to 30 rpm increased the DO in the dead zones from 4.8 to 5.53 mg/l. It confirms that increasing the rotation speed of the paddle wheel increases the flow rate of the liquid along the channel and that the response of time has no significant effect on the response of dead zone performance.

Increasing the rotational speed of the paddle wheel at a water depth of 15 cm and 35 cm improves mixing and ensures a uniform flow velocity along the channel. This results in a higher DO and fewer dead zones. Especially at a depth of 35 cm, a rotation speed of more than 30 rpm is required to minimize dead zones. If you increase the rotation speed of the paddle wheel at an optimum depth, the dead zones in the open pond are generally reduced due to the slower movement of liquid per unit of time and the better homogenization of the water layers. The flow rate of the water is directly related to the rotation speed of the paddle wheel, which means that as the rotation speed increases, the percentage of dead zones decreases. For example, if the speed of the paddle wheel increased from 10 to 30 rpm, the dead zones will decrease from 21.05 % to 9.16 %. Previous research on the effects of paddlewheel rotation speed in a raceway pond has shown that under similar conditions and at a rotation speed of 35 rpm with a six-bladed curved impeller, the dead zones are 13.4 %. By increasing the rotation speed of the impeller to 45 rpm, the dead zones were reduced to 4.16 % [37]. In another study, maintaining a rotation speed of 30 rpm and optimizing the pond dimensions (length to width ratio of 2.5) reduced the dead zones from 18 % to 3 % [19]. Sompech et al. [28]reported a 6.7 % reduction in dead zones using computational fluid dynamics (CFD) simulations and an eight-bladed flat impeller under similar conditions.

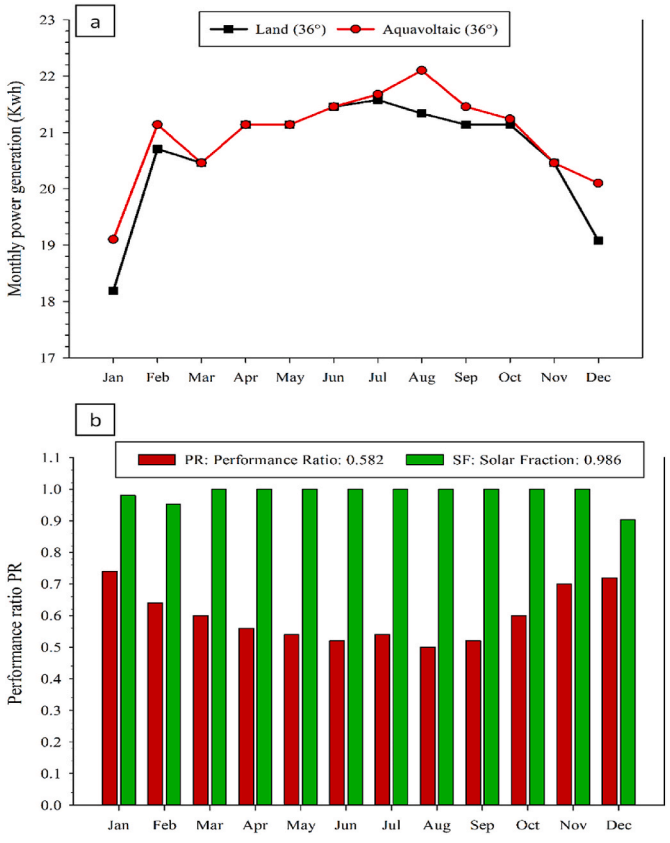


**Fig. 7.** **(a)** Results of the simulations for electricity generation, **(b)** solar fraction and power ratio.

### 3.2.2. *Optimal conditions for maximizing DO in microalgae cultivation*

As presented in equation 17, the mathematical model of the response surface was used to investigate the significant effects of the input variables on the output response (DO). To optimize the production conditions for microalgae cultivation in open raceway ponds, an optimization study was carried out using the Design Expert V13 software. The boundary conditions for the objective response were determined based on the values listed in Table 3. In the context of the aquavoltaic system study described the assignment of weights for the objective response, such as DO, can indeed play a crucial role in the optimization process. The significance level of the original response, in this case, the DO in the water, helps determine how much importance or priority should be given to this parameter during optimization.

As shown in Table 3, the desirability based on the optimal points of the input variables of the aquavoltaic system, and the applied rules is 93.9 %. It was clearly established that the optimal conditions for maximum DO are a rotation speed of 30 rpm, a water depth of more than 25 cm and a response time of 1.5 h. The results of the study show that the rotation speed of the paddle wheel has the greatest influence on the DO in the water. Therefore, it could be beneficial in the optimization process to assign a higher weight to the rotation speed parameter to ensure that the system operates under optimal conditions for microalgae production. When also considering the effects of water depth and reaction time on DO and dead zones in the pond, it is also important to assign an appropriate weighting to these parameters. By balancing the weighting of the different parameters based on their importance, the optimization process can be tailored to effectively achieve the desired results.

### 3.3. *Electric performance evaluation of the aquavoltaic system*

In this study, crystalline silicon PV module was used, which were installed together with metal structures and cables at specific locations. Both the ground-mounted reference PV module and the PV module above the open raceway pond were a 100 W module. The modules were installed at an angle of 36° to the horizon for comparison purposes. Fig. 6a shows a comparison of power generation between the ground-mounted module and the aquavoltaic module over the course of a single test day (May 15, 2023). In the morning, the power production of the ground-mounted PV module was slightly better, but the difference was minimal. After 12:30 p.m., however, the module of the aquavoltaic

**Table 3**
Optimal conditions for maximum oxygen content for the production of microalgae.

| Parameter | Goal | Lower limit | Upper limit | Optimum conditions for DO | Desirability |
|---|---|---|---|---|---|
| A: depth (cm) | is in range | 15 | 35 | 30.769 | |
| B: rotational speed (rpm) | is in range | 10 | 30 | 30 | |
| C: reaction time (h) | is in range | 0.5 | 1.5 | 1.489 | |
| DO level (mg/l) | maximize | 5.04 | 6.9 | 6.841 | 0.939 Selected |
| DO level in dead zone (mg/l) | is target = 5 | 5 | 5.5 | 5.054 | |

system showed a relatively higher power generation.

The daily electricity production of the ground-mounted reference PV module was 452 Wh, while the aquavoltaic system produced 459 Wh. In general, both the land-mounted module and the module mounted above the open raceway pond for microalgae production showed comparable electricity production throughout the day. Fig. 6a and b shows the comparison of the average daily and monthly electricity generation between the aquavoltaic system module, and the reference PV module installed on the ground on May 15 and from May to July 2023 respectively.

The performance ratio of the aquavoltaic system to the ground-mounted reference module was 101 % in May, 101 % in June, and 102 % in July. As mentioned earlier, there is an imperceptible difference between the electricity generation of the aquavoltaic system module and the land reference module. The electricity production by the aquavoltaic system module in May and June was like the ground-mounted reference module, while it was slightly higher in July. However, it is likely that the cooling effect of the water on the temperature of the module is all the more pronounced the closer the module is positioned to the water surface and the larger the pond with the open raceways is. This cooling effect can potentially improve the power generation performance compared to the reference module on land. However, further investigation and evaluation is required to confirm this.

Both systems were simulated with the PVsyst 7.1 software in order to forecast the annual power generation of the modules of the ground-mounted and aquavoltaic systems. The meteorological data came from METEONORM 7.3 and the necessary calculations for the design of the PV system were carried out. The aim of the simulation was to evaluate the electricity production of the modules of the aquavoltaic system over a year and to compare it with that of a ground-mounted module (see Fig. 7 a&b). The margin of error for the power prediction of the PV modules was 4.71 %, indicating a reliable power prediction on a test day (May 10, 2023). As shown in Fig. 7a, the power generation rate of the aquavoltaic modules was equal to or higher than that of the ground-mounted PV modules every month. The presence of water in the open ponds during the hot season had a positive impact on the module output due to the cooling effect. The largest increase in output was recorded in July, August and September, which coincide with the peak solar radiation periods. Nevertheless, the total annual electricity generation rates were similar, with the aquavoltaic modules generating 249 kWh and the ground-mounted modules 246 kWh.

This result confirms that the power generation of the aquavoltaic system over a short period of time is comparable to that of an outdoor module and that the water environment does not significantly affect the efficiency of the solar module. Unlikely, in prior research, where the concept and design of an aquavoltaic system for simultaneously harvesting salt and electricity on a salt farm floor were proposed for the first time. The salt farm water body parallel system showed an annual electricity generation rate comparable to that of land-based modules with a tilt of 30° and higher than that of land-based modules with a tilt of 0° (reference module). In this research, the modules were placed under the sea salt water at a certain height. The results indicate that the cooling effect of seawater, which maintains a certain height above the module, improves the performance of PV modules more significantly than the absorption loss caused by seawater. Ultimately, the total annual electricity generation rates were comparable. It can therefore be concluded that the power generation of the salt farm module is comparable to that of conventional solar power plants [23].

Based on the simulated results and the trend of energy losses in the system, the efficiency of the PV module is determined to be 10.39 %. According to the power ratio diagram, the amount of energy produced under STC conditions (solar radiation of 1000 W/m$^2$ and panel temperature of 25 °$C$) during the year, i.e. in each month, represents 58.2 % of the load required by the consumer (See Fig. 7b). This required load corresponds to 249 kWh. However, a solar fraction (SF) of 98.6 % indicates how close the energy supplied comes to the consumer's demand in the photovoltaic system. In general, the energy supplied in the photovoltaic system should be slightly higher than the energy required, and the closer this percentage ratio is to one, the more cost-effectively the system can meet the consumer's energy needs. The increase in the energy supplied requires higher costs for the photovoltaic system.

### 3.4. Cost analysis of the aquavoltaic system

The economic viability of aquavoltaic systems depends on a comprehensive cost analysis. This section addresses the financial aspects of deploying such systems, i.e. initial investment costs, operation and maintenance costs and potential revenue streams. In this section, the economic analysis of the developed aquavoltaic systems considering the cultivation of algae species Spirulina is presented. The costs of the different components of the aquavoltaic system in this study are shown in Table 3A. Also, the main parameters used for the economic analysis are shown in Table 4A.

The total price of the device was calculated at around 320 USD. Considering that the electricity consumed by the system is generated by the integrated PV panel and there is no cost for electricity, the only significant costs of the system are the initial construction costs, annual costs (water and fertilizer) and maintenance of the system. With a monthly production volume of dry microalgae of 10 g/month, the price for each gram is calculated at 5 USD. As can be seen in Fig. 8, the intersection of the yield and cost graphs is the point of total return on investment, which is reached in less than 8 months and then enters the profit phase. After passing the point of return on investment by applying the maintenance costs of the aquavoltaic system after 14 months, a profit of 204.68 % is achieved. The cost per liter of treated unit was estimated by Ref. [38]);

$$CPL = \frac{Total\ Annualized\ Cost}{Yearly\ Average\ Production} \tag{13}$$

$$Total\ Annualized\ Cost = Fixed\ Annual\ Cost + Annual\ Operation\ \&\ Maintenance\ Cost + Annual\ Cost$$

The total annual cost of Spirulina produced with the aquavoltaic system is 398 USD, the average annual production of Spirulina is 120 g equivalent 600 USD and the cost per liter (CPL) for Spirulina produced with the aquavoltaic system is 0.7133 USD/g. The production cost of Spirulina with the non-aquavoltaic system is 7 % higher than that of Spirulina produced with the aquavoltaic system due to the use of non-solar electricity. The CPL for Spirulina produced with a non-aquavoltaic system is 0.6633 USD/g. Fig. 9 illustrates the effects of lifespan, interest rate, and Spirulina production with aquavoltaic and non-aquavoltaic systems on the price of Spirulina. According to this figure, the cost of Spirulina produced with the aquavoltaic system in the fifth year is 0.4975 USD/g at an interest rate of 5 % and 0.331 USD/g at an interest rate of 10 %. Similarly, the cost of Spirulina produced with the non-aquavoltaic system in the fifth year will be 0.535 USD/g at an interest rate of 5 % and 0.356 USD/g at an interest rate of 10 %. This indicates that a decrease in the interest rate from 10 % to 5 % increases the cost of Spirulina production for both methods over the 5-year period. Additionally, the cost of Spirulina produced with the aquavoltaic system is lower than that of Spirulina produced with the non-aquavoltaic system at both interest rates.

The financial payback period for Spirulina production, considering annual variable costs, selling price, and annual production, was estimated for both aquavoltaic and non-aquavoltaic methods. The effect of the selling price and the type of production method on the payback period per unit is shown in Fig. 8A. The results show that if Spirulina is sold at its maximum production cost, the investment can be recovered in 0.36 years for aquavoltaic and 0.39 years for non-aquavoltaic production. The price of Spirulina on the market is between 1 USD/g and 6 USD/g, depending on the quality and the brand of the producing

**Table 4**
Comparative analysis of microalgae cultivation system parameters and performance.

| Parameter | Current Study | [14] | [19] | [9] | [20] | [21] | [37] |
|---|---|---|---|---|---|---|---|
| Dead zone percentage (%) | 9.22 | – | 3 | – | – | – | 13.4 to 4.16 |
| Mixer Speed (rpm) | 30 | – | 0.15–0.30 m/s (velocity) | – | – | – | 35, 40, 45 |
| Fluid Depth (cm) | 15 | – | – | – | – | – | – |
| Dissolved Oxygen (mg/l) | 6.841 | – | – | – | 6-7 | 5.5–5.6 | – |
| Shading Effect | 5 °C temp reduction | Reduced temperature fluctuations | – | Cooler microclimates | – | – | – |
| Solar Energy Integration | 98.6 % energy needs met | Advantageous alternative to shading nets | – | Reduces water evaporation, increases PV efficiency | – | – | – |

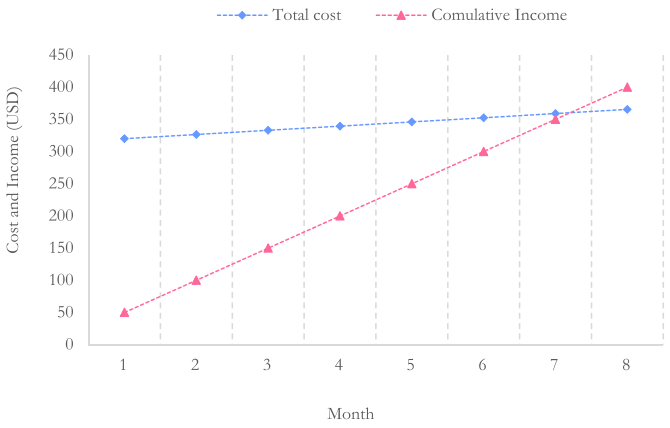


**Fig. 8.** The diagram of the investment return point of the aquavoltaic system.

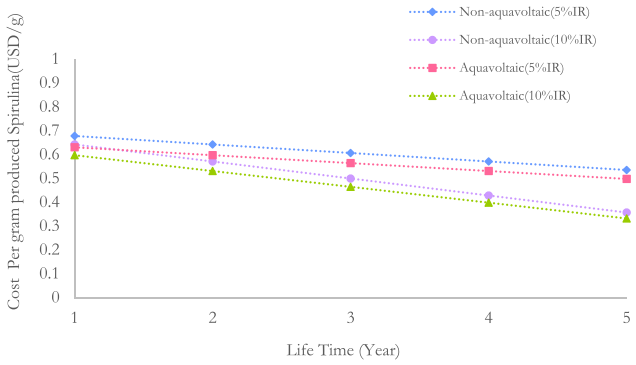


**Fig. 9.** Impact of lifetime, salinity, and interest rate on Spirulina's cost produced by the aquavoltaic and non-aquavoltaic unit.

company. This analysis shows that at a price of over USD 4/g, the financial payback falls below one year.

### 3.5. Comparison of key findings with literature

Table 4 compares the main results of this study with those available in the relevant literature and shows the effectiveness and efficiency of the application of different parameters used in the microalgae culture system in aquavoltaic setups. This comparison highlights the importance of integrating solar energy, optimized system design and environmental conditions to improve both the sustainability and productivity of aquaculture systems.

In the present study, a dead zone percentage of 9.22 % is obtained from the balance between mixer speed, liquid depth and system components, which competes with similar studies. Compared to other studies, such as Bautista-Monroy et al. [4], which reported a higher dead zone of 13.47 %, the system in the current study was more efficient. The constant agitator speed of 30 rpm in all studies suggests that this is an optimal speed to minimize dead zones. The depth of the liquid also appears to influence the percentage of dead zones, with a depth of 15 cm contributing to effective performance in the current study. The system in the present study used 4 flat vanes with a central baffle, in contrast to the 6 curved vanes used by Bautista-Monroy et al. [4] and Hadiyanto et al. [19], both of which resulted in a higher percentage of dead zones. This indicates that the type of blades and the design of the system have a significant impact on the mixing efficiency and overall performance of the aquavoltaic system.

In the current study, a DO value of 6.841 mg/l was achieved, which is within the optimal range of 6–7 mg/l reported by Lauguico et al. [20] and slightly exceeds the 5.5–5.6 mg/l predicted by Amin et al. [21] using machine learning techniques. These results highlight the ability of the system to maintain adequate oxygen supply, which is critical for microalgae health and productivity. In addition, the solar energy system in this study met 98.6 % of the aquaculture facility's energy needs, which is consistent with the findings of Vo et al. [6] and Matulić et al. [9], who emphasize the benefits of solar energy in improving the sustainability and efficiency of aquaculture facilities. This comparative analysis shows that the approach of this study is consistent with current findings from the literature while offering significant benefits in optimizing microalgae farming through strategic system design and the integration of renewable energy sources.

## 4. Conclusion

Integrating solar electricity generation with water management for microalgae cultivation, aquavoltaic systems can contribute to reducing energy consumption, maximizing land use efficiency, and controlling evaporation during dry periods. This integrated approach offers a practical solution for improving the overall efficiency and productivity of microalgae production systems. In this study, an aquavoltaic system consisting of an off-grid photovoltaic system and an open raceway pond was designed and constructed to simultaneously generate solar power and meet the energy needs of the small-scale microalgae cultivation system. From the experimental results, it was found that with a water depth of 30 cm and 91.05 % shading by the solar panels on the open pond, a temperature difference of 5 $^{\circ}C$ is created between the ambient and the water in the pond. The significant reduction in water temperature prevents the pH values from dropping and keeps them in the range of 6.5–7.5 ppm. This effectively shows that shading has a significant impact on controlling the temperature and pH range in the microalgae production pond. Considering the RSM analysis, the maximum DO was measured at 6.9 mg/l at a rotation speed of 20 rpm and a water depth of 25 cm. In addition, the percentage of dead zones at a water depth of 31 cm decreased from 21 % to 9.16 % when the rotation speeds of 10 and 30 rpm were increased. Under optimal conditions, the DO level was

measured at 6.841, representing a 61 % increase compared to the DO levels observed at the same temperature and constant depth in a non-mixed aquatic environment. These results confirm that at optimum water depth, increasing the rotation speed of the mechanical paddle wheel increases the DO in the water. The optimum conditions for DO were recorded at a rotation speed of 30 rpm, a water depth of 31 cm and a reaction time of 1.5 h, with a desirable percentage of 93.9 %. Finally, the simulation results showed that by adding a 100 Wp solar panel connected in series and connecting three 60 Ah batteries in series, the photovoltaic system would be able to cover 98.6 % of the aquaculture facility's electricity needs throughout the year. It is worth noting that the installation of pond modules is associated with higher costs due to humidity, limited accessibility, and maintenance problems. To perform economic analysis, it was assumed that Spirulina algae is cultivated within the system. The results indicated that the production cost of Spirulina with the non-quavoltaic system is 7 % higher than the aquavoltaic system due to the use of non-solar electricity. Also, the cost of Spirulina produced with the aquavoltaic system in the fifth year was calculated at 0.4975 USD/g at a %5 interest rate and 0.331 USD/g at a % 10 interest rate. In addition, the CPL for Spirulina produced with the aquavoltaic system was calculated at 0.7133 USD/g.

## CRediT authorship contribution statement

**Hooman Pirtaj Hamedani:** Writing – original draft, Validation, Software, Methodology, Formal analysis, Data curation. **Shiva Gorjian:** Writing – review & editing, Visualization, Supervision, Resources, Project administration, Funding acquisition, Conceptualization. **Barat Ghobadian:** Writing – review & editing, Visualization, Supervision, Resources. **Hamed Mokhtarzadeh:** Writing – original draft, Software, Investigation, Formal analysis, Data curation.

## Declaration of competing interest

The authors declare that they have no known competing financial interests or personal relationships that could have appeared to influence the work reported in this paper.

## Data availability

The data that has been used is confidential.

## Appendix A. Supplementary data

Supplementary data to this article can be found online at https://doi.org/10.1016/j.rineng.2024.102919.

## References


[1] J. Bostock, B. McAndrew, R. Richards, K. Jauncey, T. Telfer, K. Lorenzen, D. Little, L. Ross, N. Handisyde, I. Gatward, Aquaculture: global status and trends, Phil. Trans. Biol. Sci. 365 (2010) 2897–2912.

[2] M.J. MacLeod, M.R. Hasan, D.H.F. Robb, M. Mamun-Ur-Rashid, Quantifying greenhouse gas emissions from global aquaculture, Sci. Rep. 10 (2020) 11679.

[3] T. Sampantamit, L. Ho, W. Van Echelpoel, C. Lachat, P. Goethals, Links and trade-offs between fisheries and environmental protection in relation to the sustainable development goals in Thailand, Water (Basel) 12 (2020) 399, https://doi.org/10.3390/w12020399.

[4] S.S. Bautista-Monroy, E.A. Chávez-Urbiola, R. Ortega-Palacios, A. González-Sánchez, C.A. Gómez-Aldapa, O. Rodríguez-Nava, J.C. Salgado-Ramírez, A. Cadena-Ramírez, Insights of raceway bioreactor scale-up: effect of agitation on microalgae culture and reduction of the liquid medium speed, Appl. Sci. 12 (2022), https://doi.org/10.3390/app12031513.

[5] M. Imani, H. Fakour, S.-L. Lo, M.-H. Yuan, C.-K. Chen, S. Mobasser, I. Muangthai, Aquavoltaics feasibility assessment: synergies of solar PV power generation and aquaculture production, Water (Basel) 15 (2023) 987, https://doi.org/10.3390/w15050987.

[6] T.T.E. Vo, H. Ko, J.-H. Huh, N. Park, Overview of solar energy for aquaculture: the potential and future trends, Energies 14 (2021) 6923, https://doi.org/10.3390/en14216923.

[7] C. Hermann, F. Dahlke, U. Focken, M. Trommsdorff, Aquavoltaics: dual use of natural and artificial water bodies for aquaculture and solar power generation, in: Solar Energy Advancements in Agriculture and Food Production Systems, Elsevier, 2022, pp. 211–236, https://doi.org/10.1016/B978-0-323-89866-9.00009-2.

[8] S. Gorjian, S. Minaei, L. MalehMirchegini, M. Trommsdorff, R.R. Shamshiri, Applications of solar PV systems in agricultural automation and robotics, in: S. Gorjian, A. Shukla (Eds.), Photovoltaic Solar Energy Conversion, Elsevier, London, 2020, pp. 191–235, https://doi.org/10.1016/B978-0-12-819610-6.00007-7.

[9] D. Matulić, Ž. Andabaka, S. Radman, G. Fruk, J. Leto, J. Rošin, M. Rastija, I. Varga, T. Tomljanović, H. Čeprnja, M. Karoglan, Agrivoltaics and aquavoltaics: potential of solar energy use in agriculture and freshwater aquaculture in Croatia, Agriculture 13 (2023) 1447, https://doi.org/10.3390/agriculture13071447.

[10] G. Francis, H.P.S. Makkar, K. Becker, Antinutritional factors present in plant-derived alternate fish feed ingredients and their effects in fish, Aquaculture 199 (2001) 197–227, https://doi.org/10.1016/S0044-8486(01)00526-9.

[11] T. Seong, Y. Uno, R. Kitagima, N. Kabeya, Y. Haga, S. Satoh, Microalgae as main ingredient for fish feed: non-fish meal and non-fish oil diet development for red sea bream, Pagrus major, by blending of microalgae Nannochloropsis, Chlorella and Schizochytrium, Aquacult. Res. 52 (2021) 6025–6036, https://doi.org/10.1111/are.15463.

[12] K.P. Sandeep, K.P. KumaraguruVasangam, P. Kumararaja, J. Syama Dayal, G. B. Sreekanth, K. Ambasankar, K.K. Vijayan, Microalgal diversity of a tropical estuary in south India with special reference to isolation of potential species for aquaculture, J. Coast Conserv. 23 (2019) 253–267, https://doi.org/10.1007/s11852-018-0655-4.

[13] J.C.M. Pires, M.C.M. Alvim-Ferraz, F.G. Martins, Photobioreactor design for microalgae production through computational fluid dynamics: a review, Renew. Sustain. Energy Rev. 79 (2017) 248–254.

[14] S. Gorjian, F. Kamrani, O. Fakhraei, H. Samadi, P. Emami, Emerging applications of solar energy in agriculture and aquaculture systems, in: Solar Energy Advancements in Agriculture and Food Production Systems, Elsevier, 2022, pp. 425–469, https://doi.org/10.1016/B978-0-323-89866-9.00008-0.

[15] F.G. Acién, E. Molina, A. Reis, G. Torzillo, G.C. Zittelli, C. Sepúlveda, J. Masojídek, Photobioreactors for the production of microalgae, in: Microalgae-Based Biofuels and Bioproducts, Elsevier, 2017, pp. 1–44, https://doi.org/10.1016/B978-0-08-101023-5.00001-7.

[16] F. Bux, Y. Chisti, Algae Biotechnology. Products and Processes, vol. 344, Green Energy and Technology, 2016, https://doi.org/10.1007/978-3-319-12334-9.

[17] Y. Chisti, Raceways-based production of algal crude oil, Greenpeace 3 (2013) 195–216, https://doi.org/10.1515/green-2013-0018.

[18] S. Gorjian, R. Singh, A. Shukla, A.R. Mazhar, in: S. Gorjian, A.B.T.-P.S.E.C. Shukla (Eds.), Chapter 6 - On-Farm Applications of Solar PV Systems, Academic Press, 2020, pp. 147–190, https://doi.org/10.1016/B978-0-12-819610-6.00006-5.

[19] H. Hadiyanto, S. Elmore, T. Van Gerven, A. Stankiewicz, Hydrodynamic evaluations in high rate algae pond (HRAP) design, Chem. Eng. J. 217 (2013) 231–239, https://doi.org/10.1016/j.cej.2012.12.015.

[20] S. Lauguico, R. Concepcion, R.R. Tobias, J. Alejandrino, D. Macasaet, E. Dadios, Indirect measurement of dissolved oxygen based on algae growth factors using machine learning models, in: 2020 IEEE 8th R10 Humanitarian Technology Conference (R10-HTC), IEEE, 2020, pp. 1–6, https://doi.org/10.1109/R10-HTC49770.2020.9357014.

[21] S. Amin, F. Cuomo, M. Kamal, Comparative analysis of data driven prediction modeling strategies for aquaculture healthcare, in: 2021 International Conference on Innovative Computing (ICIC), IEEE, 2021, pp. 1–6.

[22] P.-A. Château, R.F. Wunderlich, T.-W. Wang, H.-T. Lai, C.-C. Chen, F.-J. Chang, Mathematical modeling suggests high potential for the deployment of floating photovoltaic on fish ponds, Sci. Total Environ. 687 (2019) 654–666, https://doi.org/10.1016/j.scitotenv.2019.05.420.

[23] B. Kim, S. Lee, S. Kang, M. Jeong, G.H. Gim, J. Park, C. Lim, Aquavoltaic system for harvesting salt and electricity at the salt farm floor: concept and field test, Sol. Energy Mater. Sol. Cell. 204 (2020) 110234, https://doi.org/10.1016/j.solmat.2019.110234.

[24] J. Hu, K. Teng, C. Li, X. Li, J. Wang, P.D. Lund, Review of recent water photovoltaics development, Oxford Open Energy 2 (2023), https://doi.org/10.1093/ooenergy/oiad005.

[25] K. Trapani, D.L. Millar, The thin film flexible floating PV (T3F-PV) array: the concept and development of the prototype, Renew. Energy 71 (2014) 43–50, https://doi.org/10.1016/j.renene.2014.05.007.

[26] T.T.E. Vo, S.-M. Je, S.-H. Jung, J. Choi, J.-H. Huh, H.-J. Ko, Review of photovoltaic power and aquaculture in desert, Energies 15 (2022) 3288, https://doi.org/10.3390/en15093288.

[27] Y.-C. Cheng, T.S. Li, H.L. Su, P.C. Lee, H.-M.D. Wang, Transdermal delivery systems of natural products applied to skin therapy and care, Molecules 25 (2020) 5051.

[28] K. Sompech, Y. Chisti, T. Srinophakun, Design of raceway ponds for producing microalgae, Biofuels 3 (2012) 387–397, https://doi.org/10.4155/bfs.12.39.

[29] J. Mayorga, R. Chávez, O. Mayorga, J. Delgado-Linares, R. Sánchez, G. Delgado-Linares, Escalamiento del reactor del proceso de coquización retardada, Ciencia e Ingeniería 35 (2014) 147–155.

[30] R. King, Mechanical Aspects of Mixing, Mixing in the Process Industries. Reed Educational and Professional Publishing Ltd, 1997, https://doi.org/10.1016/b978-075063760-2/50034-2.

[31] A.W. Nienow, M.F. Edwards, N. Harnby, Mixing in the Process Industries, Butterworth-Heinemann, 1997.

[32] R.S. Khurmi, J.K. Gupta, A Textbook of Machine Design, S. Chand publishing, 2005.

[33] M. Nassiri Mahallati, Chapter 9 - advances in modeling saffron growth and development at different scales, in: A. Koocheki, M.B.T.-S. Khajeh-Hosseini (Eds.), Woodhead Publishing Series in Food Science, Technology and Nutrition, Woodhead Publishing, 2020, pp. 139–167, https://doi.org/10.1016/B978-0-12-818638-1.00009-5.

[34] J.G. Carton, A.G. Olabi, Design of experiment study of the parameters that affect performance of three flow plate configurations of a proton exchange membrane fuel cell, Energy 35 (2010) 2796–2806, https://doi.org/10.1016/j.energy.2010.02.044.

[35] P. Li, X. Gao, J. Jiang, L. Yang, Y. Li, Characteristic analysis of water quality variation and fish impact study of fish-lighting complementary photovoltaic power station, Energies 13 (2020) 4822.

[36] K.Y. Benyounis, A.G. Olabi, M.S.J. Hashmi, Multi-response optimization of CO2 laser-welding process of austenitic stainless steel, Opt Laser. Technol. 40 (2008) 76–87, https://doi.org/10.1016/j.optlastec.2007.03.009.

[37] Bautista-Monroy, J.C. Salgado-Ramírez, A. Téllez-Jurado, M.R. Ramírez-Vargas, C. A. Gómez-Aldapa, K.J. Pérez-Viveros, S.A. Medina-Moreno, A. Cadena-Ramírez, Hydrodynamic characterization in a raceway bioreactor with different stirrers, Rev. Mex. Ing. Quim. 18 (2019) 605–619.

[38] K.R. Ranjan, S.C. Kaushik, Economic feasibility evaluation of solar distillation systems based on the equivalent cost of environmental degradation and high-grade energy savings, Int. J. Low Carbon Technol. 11 (2014) 8–15, https://doi.org/10.1093/ijlct/ctt048.